JOC Article

Photodissociation of Acetic Acid in the Gas Phase: An ab Initio Study

Wei-Hai Fang* and Ruo-Zhuang Liu

Department of Chemistry, Beijing Normal University, Beijing 100875, P. R. China

Xuming Zheng and David Lee Phillips*

Department of Chemistry, The University of Hong Kong, Pokfulam Road, Hong Kong, P. R. China

fangwh@bnu.edu.cn

Received May 29, 2002

Photodissociation of acetic acid in the gas phase was investigated using ab initio molecular orbital methods. The stationary structures on the ground-state potential energy surfaces were mainly optimized at the MP2 level of theory, while those on the excited-state surfaces were determined by complete active space SCF calculations with a correlation-consistent basis set of cc-pVDZ. The reaction pathways leading to different photoproducts are characterized on the basis of the computed potential energy surfaces and surface crossing points. The calculations reproduce the experimental results well and provide additional insight into the mechanism of the ultraviolet photodissociation of acetic acid and related compounds.

I. Introduction

Molecular photodissociation reactions have long been regarded as a challenging area of chemical physics. These reactions are relevant to atmospheric chemistry, biological systems, and many other processes.[1−5] Photodissociation reactions of carbonyl and carboxylic compounds have been the subject of numerous experimental investigations[6−17] including measurements of the energy distributions of the resulting photoproducts, the relative quantum yields of different fragments, and the fragment anisotropies. Due to the great diversity of possible reaction pathways as well as the complexity of the product mixtures, it is currently difficult for experiments to provide detailed mechanisms of the photodissociation. In principle, quantum chemical ab initio calculations of the potential energy surfaces (PES) of different pathways should help clarify the dissociation mechanisms. However, such a theoretical study is not trivial and would require considerable computational effort. Calculations to date have mainly been performed for relatively small molecules, such as H_2CO,[18] HONO,[19] HNCO,[20] CH_3CHO,[21] CH_2CHCHO,[22,23] $CH_2CHCOOH$,[24] and so on.[25,26]

Acetic acid is one of the simplest carboxylic acids so that its underlying decomposition dynamics have been extensively investigated from viewpoints of both experiment and theory. Early studies on the gas-phase unimolecular decomposition[27−29] of acetic acid identified two molecular channels given by eqs 1 and 2.

(1) Cantor, C. R.; Schimmel, P. R. *Biophysical Chemistry I*; Freemann: San Francisco, CA, 1980.
(2) Andreae, M. O.; Talbot, R. W.; Andreae, T. W.; Harriss, R. C. *J. Geophys. Res.* **1988**, *93*, 1616.
(3) Keene, W. C.; Galloway, J. N.; Holden, J. D. *J. Geophys. Res.* **1983**, *88*, 5122.
(4) Grosjean, D. *Atmos. Environ., Part A* **1992**, *26*, 3279.
(5) Kesselmeier, J.; Bode, K.; Gerlach, C.; Jork, E.-M. *Atmos. Environ.* **1998**, *32*, 1765.
(6) Huang, C.-K.; Chien, V.; Chen, I.-C. *J. Chem. Phys.* **2000**, *112*, 1797.
(7) Furlan, A.; Scheld, H. A.; Huber J. R. *J. Phys. Chem. A* **1999**, *104*, 1920.
(8) Yoon, M.-C.; Choi, Y.-S.; Kim, S.-K. *J. Chem. Phys.* **1999**, *110*, 7185.
(9) Zhong, Q.; Poth, L.; Castleman, A. W., Jr. *J. Chem. Phys.* **1999**, *110*, 192.
(10) Owrutsky, J. C.; Baronavski, A. P. *J. Chem. Phys.* **1999**, *111*, 7329.
(11) Hunnicutt, S. S.; Waits, L. D.; Guest, J. A. *J. Phys. Chem.* **1989**, *93*, 5188.
(12) Hunnicutt, S. S.; Waits, L. D.; Guest, J. A. *J. Phys. Chem.* **1991**, *95*, 562.
(13) Peterman, D. R.; Daniel, R. G.; Horwitz, R. J.; Guest, J. A. *Chem. Phys. Lett.* **1995**, *236*, 564.
(14) Singleton, D. L.; Paraskevopoulos, G.; Irwin, R. S. *J. Am. Chem. Soc.* **1989**, *111*, 5248.
(15) Singleton, D. L.; Paraskevopoulos, G.; Irwin, R. S. *J. Phys. Chem.* **1990**, *94*, 695.
(16) Naik, P. D.; Upadhyaya, H. P.; Kumar, A.; Sapre, A. V.; Mittal, J. P. *Chem. Phys. Lett.* **2001**, *340*, 116.
(17) Kwon, H. T.; Shin, S. K.; Kim, S. K.; Kim, H. L. *J. Phys. Chem. A* **2001**, *105*, 6775.
(18) Yamaguchi, Y.; Wesolowski, S. S.; Van Huis, T;. Schaefer H. F., III *J. Chem. Phys.* **1998**, *108*, 5281.
(19) Cotting, R.; Huber, J. R. *J. Chem. Phys.* **1996**, *104*, 6208.
(20) Cui, Q.; Morokuma, K. *J. Chem. Phys.* **1998**, *108*, 1452.
(21) King, R. A.; Allen, W. D.; Schaefer H. F., III *J. Chem. Phys.* **2000**, *112*, 5585 and references therein.
(22) Reguero, M.; Olivucci, M.; Bernardi, F.; Robb, M. A. *J. Am. Chem. Soc.* **1994**, *116*, 2103.
(23) Fang, W.-H. *J. Am. Chem. Soc.* **1999**, *121*, 8376.
(24) Fang, W.-H.; Liu, R.-Z. *J. Am. Chem. Soc.* **2000**, *122*, 10886.
(25) Yamamoto, N.; Olivucci, M.; Celani, P.; Bernardi, F.; Robb, M. A. *J. Am. Chem. Soc.* **1998**, *120*, 2391.
(26) Wilsey, S.; Houk, K. N.; Zewail, A. H. *J. Am. Chem. Soc.* **1999**, *121*, 5772.
(27) Bamford, C. H.; Dewar, M. J. S. *J. Chem. Soc.* **1949**, 2877.
(28) Blake, P. G.; Jackson, G. E. *J. Chem. Soc. B* **1968**, 1153.
(29) Blake, P. G.; Jackson, G. E. *J. Chem. Soc. B* **1969**, 94.

10.1021/jo020356o CCC: $22.00
Published on Web 10/30/2002

$$CH_3COOH \rightarrow CH_4 + CO_2 \quad (1)$$

$$\rightarrow CH_2CO + H_2O \quad (2)$$

Mackie and Doolan[30] and Satio et al.[31] measured the decomposition of acetic acid in a shock tube and the activation energies were estimated to be in the range 6−73 kcal/mol for reaction 1 and 65−73 kcal/mol for reaction 2. The H_2O and CO_2 relative emission intensities and RRKM calculations by Butkovskaya et al.[32] suggested that the gas-phase unimolecular decomposition of CH_3COOH proceeds through the two competing pathways (1) and (2) with approximately 2 times higher probability for H_2O formation. The threshold energies for the two reactions must be less than 70 kcal/mol. The infrared multiphoton dissociation[33] of acetic acid in a rotating source molecular beam machine was studied by photofragment translational spectroscopy. Carbon dioxide and methane were observed for the first time as products from dissociation under collisionless conditions.[33]

Besides the thermal decomposition mentioned above, experimentalists have long been interested in the photodissociation reaction of acetic acid. On the basis of the stable products observed in the photolysis of acetic acid, several possible dissociation processes[34−37] were suggested as follows,

$$CH_3COOH + h\nu \rightarrow CH_3CO + OH \quad (3)$$

$$\rightarrow CH_3 + COOH \quad (4)$$

$$\rightarrow CH_3COO + H \quad (5)$$

$$\rightarrow CH_2COOH + H \quad (6)$$

No single reaction pathway was shown to be predominant in these early studies.[34−37] Recently, acetic acid has been photolyzed at 218 nm under both room-temperature and jet-cooled conditions.[11] The energy partitioning observed in the photodissociation experiment predicts the major pathway for CH_3COOH photodissociation is reaction 3 at this wavelength with no subsequent decomposition of the acetyl fragment. The acetic acid absorption at 218 and 200 nm accesses the same $^1n\pi^*$ band, and the average translational energy of OH from the 200-nm photolysis was found to be nearly the same as that for OH from the 218-nm photolysis.[12] This observation supports an exit channel barrier model for acetic acid decomposition in the gas phase. Comparison of the internal and translational energy distributions of OD ($^2\Pi$) with those of OH ($^2\Pi$) reveals the effects of isotopic substitution on the α-cleavage photodynamics of $^1n\pi^*$-excited acetic acid.[13] A pure impulsive model for the dissociation dynamics is inadequate to explain the isotopic substitution results. The primary quantum yields for formation of OH radicals in the photodissociation of the monomer and dimer of acetic acid vapor at 222 nm have been determined at two temperatures.[14,15] The quantum yield from the monomer was found to be 0.7−0.8, while the yield from the dimer is nearly zero. Very recently, Owrutsky and Baronavski[10] have performed an ultrafast photodissociation study on acetic acid using single photon deep ultraviolet excitation and mass-resolved multiphoton ionization detection to investigate subsequent unimolecular decomposition of the acetyl radical. The photodissociation dynamics of acetic acid in the gas phase has been investigated by probing the nascent photoproduct OH using laser-induced fluorescence spectroscopy.[16,17] The OH formation was confirmed to be the dominant channel[16] for 193-nm photolysis of acetic acid in the gas phase. It was concluded from the measured energy distribution and no polarization dependence that the dissociation takes place along the triplet surface with an exit channel barrier.

Acetic acid has also been the subject of many theoretical calculations. The ground-state decarboxylation and dehydration channels were first optimized at the Hartree−Fock (HF) level of theory by Ruelle et al.,[38,39] Liu et al.,[40] and Skancke.[41] The HF calculations overestimated the activation energies of the decarboxylation and dehydration by about 15 kcal/mol, as compared with the experimentally inferred values.[30−33] Recently, more sophisticated ab initio calculations at the CI[42] and CASSCF[43] levels of theory have been performed to examine the competition between decarboxylation and dehydration in the unimolecular decomposition of acetic acid and the competition between one-step and two-step mechanisms for the dehydration reaction. The calculated barriers for CH_3COOH decarboxylation and dehydration in the ground state are close to those determined by experimental measurements. To test the validity of the ab initio molecular dynamics method,[44] the thermal decarboxylation and dehydration of acetic acid have been investigated using density functional theory methods.

A great deal of experimental and computational effort has been devoted to the study of acetic acid (CH_3COOH) decomposition. However, there is no theoretical information (to our knowledge) available for the excited-state potential energy surfaces for different reaction pathways, which is required to characterize the mechanism of the CH_3COOH photodissociation. In this paper, we report an extensive ab initio calculation carried out by employing several advanced techniques. The ground- and excited-state potential energy surfaces are traced at different levels of theory. These calculated potential energy surfaces and the computed intersections between the surfaces are used to determine the most probable mechanisms leading to different photoproducts.

In addition to the elucidation of mechanistic features, this work was also motivated by the bond selective nature of photodissociation processes occurring in asymmetri-

(30) Mackie, J. C.; Doolan, K. R. *Int. J. Chem. Kinet.* **1984**, *16*, 525.
(31) Satio, K.; Sasaki, T.; Yoshinobu, I.; Imamura, A. *Chem. Phys. Lett.* **1990**, *170*, 385.
(32) Butkovskaya, N. I.; Manke, G., II; Setser, D. W. *J. Phys. Chem.* **1995**, *99*, 11115.
(33) Longfellow, C. A.; Lee, Y. T. *J. Phys. Chem.* **1995**, *99*, 15532.
(34) Ausloos, P.; Steacie, E. W. R. *Can. J. Chem.* **1955**, *33*, 1530.
(35) Burton, M. *J. Am. Chem. Soc.* **1936**, *58*, 1655.
(36) Terenin, A.; Neujmin, H. *J. Chem. Phys.* **1935**, *3*, 436.
(37) Dyne, P. J.; Style, D. W. G. *Discuss. Faraday Soc.* **1947**, *2*, 159.
(38) Puelle, P. *Chem. Phys.* **1986**, *110*, 263.
(39) Nguyen, M. T.; Puelle, P. *Chem. Phys. Lett.* **1987**, *138*, 486.
(40) Xie, J. F.; YU, J. G.; Feng, W. L.; Liu, R.-Z. *J. Mol. Struct. (THEOCHEM)* **1989**, *201*, 249.
(41) Shancke, P. N. *J. Phys. Chem.* **1992**, *96*, 8065.
(42) Nguyen, M. T.; Sengupta, D.; Raspoet, G.; Vanquickenborne, L. G. *J. Phys. Chem.* **1995**, *99*, 11883.
(43) Duan, X.; Page, M. *J. Am. Chem. Soc.* **1995**, *117*, 5114.
(44) Liu, Z. F.; Siu, C. K.; Tse, J. S. *Chem. Phys. Lett.* **1999**, *314*, 317.

cally substituted carbonyl compounds, such as acetyl halides and acetyl cyanide. An interesting feature of these photodissociation reactions is that the stronger bond, such as C−Cl and C−O bonds, cleaves preferentially over the weaker C−C bond. This has been qualitatively explained on the basis of experimental observation and consideration of the low-lying electronic configurations.[45,46] We briefly discuss this bond selective behavior for photodissociation processes of selected asymmetrically substituted carbonyl compounds using the mechanistic insight obtained from our present calculation results for the ultraviolet photodissociation of acetic acid.

II. Computational Details

Ab initio molecular orbital methods have been used to investigate the ground- and excited-state potential energy surfaces of acetic acid. The stationary structures on the ground-state surface were optimized at the MP2 and CASSCF levels of theory, while the CASSCF method was used to determine the stationary structures on the potential energy surfaces of the lowest excited triplet and singlet states. Analytical frequency computations at the CASSCF and MP2 levels were used to confirm the nature of the located critical points and to make zero-point energy corrections for the relative energies reported in the present calculations. Intersections between the S_1 and T_1 as well as the S_0 surfaces were optimized with the state-averaged CASSCF (SA-CASSCF) method (details of this method can be found in ref 47). The spin−orbit coupling calculations were carried out using a one-electron approximation for the spin−orbital coupling operator with the effective nuclear charges of Koseki et al.[48] The energy of the separated fragments was determined from a supermolecule calculation that puts both fragments at a large separation. This calculation uses the same basis set and active space as the calculation of the bound fragments. A correlation-consistent basis set of cc-pVDZ[49] was employed in these calculations. The MP2 and CASSCF computations were done using the Gaussian 98 program software packages.[50]

The CASSCF wave function used a multi-configuration SCF wave function that includes all configurations of a given spin multiplicity that can be constructed distributing a set of active electrons among a set of active orbitals. It is impossible to perform a CASSCF optimization with all valence electrons in the active space for acetic acid. Thus, the selection of the active space becomes a crucial step. In the present CASSCF optimizations, the active space is composed of eight electrons in seven orbitals, referred to as CAS(8,7) hereafter, but the active orbitals are varied with the dissociation processes. For minimum-energy structures of acetic acid in the S_0, T_1, and S_1 states, the π and π^* orbitals of the C=O moiety, the two O3 nonbonding orbitals, and the $2p_z$ orbital of O4 atom are employed as active orbitals. The other two active orbitals were selected by test CASSCF calculations, which are a linear combination of the C−C and C−O σ^* molecular orbitals. We also performed the CASSCF calculations with one of the O3 nonbonding orbitals replaced by the $2p_x$ or $2p_y$ of the O4 atom, which provides relatively high energy. For the dissociation processes that involve the C−C or C−O σ bond cleavage, the corresponding σ orbital is included in the active space for the CAS(8,7) calculation of the transition state with the O3 or O4 nonbonding orbital excluded. The active space for transition state calculations will be further elucidated in the relevant sections below.

The CASSCF method allows for the balanced representation of several states simultaneously, and can provide a reliable description of the stationary structures on the S_0, T_1, and S_1 surfaces. However, since many of the valence electrons have been treated as filled closed-shell orbitals with no recovery of correlation energy and the active electrons have only a partial recovery of correlation, the CAS(8,7) calculations may overestimate the relative energies of the stationary structures on the T_1 and S_1 surfaces. In addition, active orbitals used for equilibrium geometries are different from those employed for transition state structures, which also can cause some deviations in the calculated barrier heights. To refine the relative energies of the stationary structures, the single-point energy is calculated at the CAS+1+2 level of theory (CASSCF/MRSDCI) with the cc-pVDZ basis set. A total of 24 valence electrons and all the virtual orbitals are included in the CAS+1+2 correlation energy calculations, with the C and O 1s electrons treated as frozen core. The CAS+1+2 computations were done using MOLPRO program software packages.[51]

III. Results and Discussion

A. Unimolecular Decomposition Reactions in the Ground State. We first describe the MP2/cc-pVDZ ground-state surface and compare it with previous experimental and theoretical results. Two minimum-energy conformers, referred to as **1a**(S_0) and **1b**(S_0) in Figure 1, were found on the ground-state surface. **1a**(S_0) is more stable by 6.0 kcal/mol relative to **1b**(S_0). Isomerization between **1a**(S_0) and **1b**(S_0) involves OH rotation around the C−O single bond and a transition state [TSab(S_0)] (shown in Figure 1). The H5−O4−C2−O3 dihedral angle varies from 0.0° in **1a**(S_0) to 96.0° in TSab(S_0) and to 180.0° in **1b**(S_0). The barrier height is 12.7 kcal/mol at the MP2/cc-pVDZ level of theory relative to the **1a**(S_0) minimum, which predicts that acetic acid exists mainly in the form of **1a**(S_0) at room temperature. This is consistent with experimental observation. The **1a**(S_0) geometry was further optimized at the CAS(8,7)/cc-pVDZ level of theory. The C1−C2, C2−O3, and C2−O4 bond lengths are predicted to be respectively 1.507, 1.213, and 1.360 Å by the present CAS(8,7)/cc-pVDZ calculations, which are very close to the corresponding MP2/cc-pVDZ calculated values in Figure 1. The previous CAS(10,10)/6-31G(d) calculations[43] predicted the C1−C2, C2−O3, and C2−O4 bond lengths to be 1.527, 1.193, and 1.370 Å,

(45) Person, M. D.; Kash, P. W.; Butler, L. J. *J. Phys. Chem.* **1992**, *96*, 2021.
(46) Person, M. D.; Kash, P. W.; Butler, L. J. *J. Chem. Phys.* **1992**, *97*, 355.
(47) Bernardi, F.; Olivucci, M.; Robb, M. A. *Chem. Soc. Rev.* **1996**, *25*, 321 and references therein.
(48) Koseki, S.; Schmidt, M. W.; Gordon, M. S. *J. Phys. Chem.* **1992**, *96*, 10768.
(49) Dunning, T. H., Jr. *J. Chem. Phys.* **1989**, *90*, 1007.
(50) Frisch, M. J.; Trucks, G. W.; Schlegel, H. B.; Scuseria, G. E.; Robb, M. A.; Cheeseman, J. R.; Zakrzewski, V. G.; Montgomery, J. A., Jr.; Stratmann, R. E.; Burant, J. C.; Dapprich, S.; Millam, J. M.; Daniels, A. D.; Kudin, K. N.; Strain, M. C.; Farkas, O.; Tomasi, J.; Barone, V.; Cossi, M.; Cammi, R.; Mennucci, B.; Pomelli, C.; Adamo, C.; Clifford, S.; Ochterski, J.; Petersson, G. A.; Ayala, P. Y.; Cui, Q.; Morokuma, K.; Malick, D. K.; Rabuck, A. D.; Raghavachari, K.; Foresman, J. B.; Cioslowski, J.; Ortiz, J. V.; Baboul, A. G.; Stefanov, B. B.; Liu, G.; Liashenko, A.; Piskorz, P.; Komaromi, I.; Gomperts, R.; Martin, R. L.; Fox, D. J.; Keith, T.; Al-Laham, M. A.; Peng, C. Y.; Nanayakkara, A.; Gonzalez, C.; Challacombe, M.; Gill, P. M. W.; Johnson, B.; Chen, W.; Wong, M. W.; Andres, J. L.; Gonzalez, C.; Head-Gordon, M.; Replogle, E. S.; Pople, J. A. *Gaussian98*; Gaussian, Inc.: Pittsburgh, PA, 1998.
(51) MOLPRO is a package of ab initio programs written by Weener, H.-J.; Knowles, P. J. with contributions from Almlof, J.; Amos, R. D.; Cooper, D. L.; Deegan, M. J. O.; Dobbyn, A. J.; Eclert, E.; Elbert, S. T.; Hampel, C.; Lindh, R.; Lloyd, A. W.; Meyer, W.; Nicklass, A.; Peterson, K.; Pitzer, R.; Stone, A. J.; Taylor, P. R.; Mura, M. E.; Pulay, P.; Schutz, M.; Stoll, H.; Thorsteinsson, T.

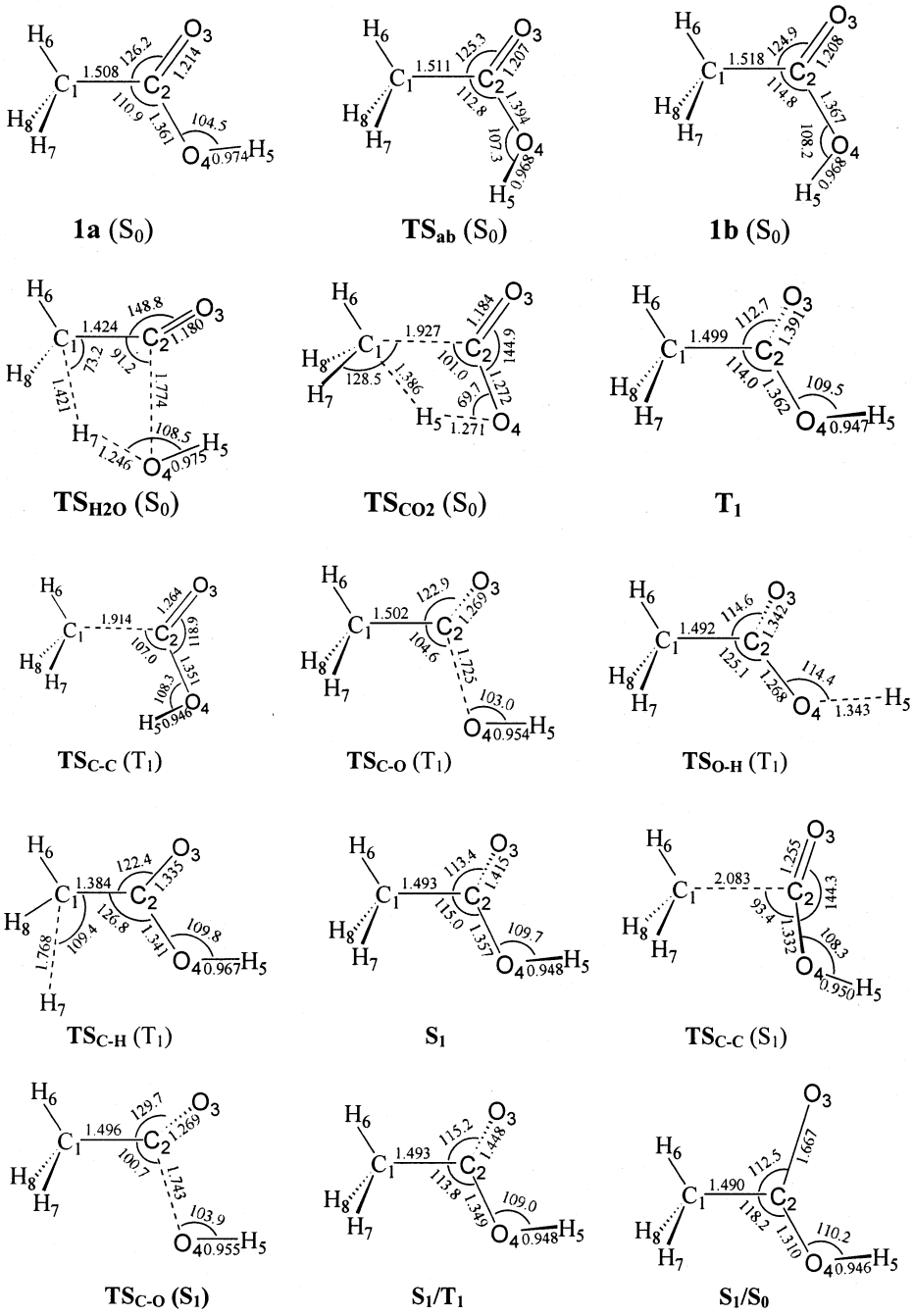

FIGURE 1. Schematic structures of the stationary points on different electronic states and the selected MP2 bond parameters for the S_0 structures and the CAS(8,7) bond parameters for the T_1 and S_1 structures are given (bond lengths in Å and bond angles in deg).

respectively. In comparison with the corresponding experimental values[52] of 1.504, 1.215, and 1.362 Å, the ground-state structure of acetic acid is well described by the CASSCF and MP2 calculations.

Examination of the **1a**(S_0) structure in Figure 1 shows that isomerization to **1b**(S_0) takes place prior decarboxylation. The decarboxylation reaction involves a 1,3-H shift of the H5 atom accompanied by a cleavage of the C−C bond. Although a nonplanar geometry was used as the initial guess, the optimized structure of the transition state [$TS_{CO2}(S_0)$] actually has a C_s symmetry with H7 and H8 lying in the symmetric plane above and below. The barrier to decarboxylation was calculated to be 67.2 kcal/mol at the MP2/cc-pVDZ level of theory and including a vibrational zero-point energy correction. This result was lower than the QCISD(TC)/6311++G(d,p)//MP2/6-31G(d,p) calculated barrier of 72 kcal/mol[42] and the CAS(10,10)/6-31G(d) value of 71.8 kcal/mol.[43] The present MP2/cc-pVDZ computations exhibit better agreement with the experimental estimation of 62−70 kcal/mol and provide a better description of the ground-state decarboxylation reaction of acetic acid.

(52) Van Eijck, B. P.; Van Opheusden, J.; Van Schaik, M. M. M.; Van Zoeren, E. *J. Mol. Spectrosc.* **1981**, *86*, 465.

Dehydration is another important channel for the CH_3COOH dissociation in the ground state. The one-step dehydration process involves a 1,3-shift of H6 from C1 to O4, in addition to the C2−O4 cleavage. Since the H6 atom is in the trans position of the O−H group with respect to the C−C single bond, the H6 transfer is accompanied by a rotation of the CH_3 group. A nonplanar transition state, $TS_{H_2O}(S_0)$ in Figure 1, was optimized at the MP2/cc-pVDZ level of theory. The displacement vector associated with the imaginary mode of $TS_{H_2O}(S_0)$ was identified as $0.16R_{C1-C2} - 0.53R_{C1-H6} + 0.60R_{O4-H6} - 0.08A_{H6-C1-C2} - 0.32A_{O4-H6-C1}$, and this clearly shows that $TS_{H_2O}(S_0)$ is the transition state governing the CH_3COOH decomposition into CH_2CO and H_2O fragments. With respect to the zero level of **1a**(S_0), the barrier to dehydration is 71.7 kcal/mol (as shown in Figure 2a). The MP2/cc-pVDZ calculated barrier is a little lower than those found from previous calculations (the CAS(10,10)/6-31G(d) value of 76.4 kcal/mol[43] and the QCISD(TC)/6-311++G(d,p)//MP2/6-31G(d,p) value of 75.8 kcal/mol[42]) and close to a recent experimental estimation[32] that the threshold energy for dehydration reaction must be less than 70 kcal/mol.

As pointed out in previous calculations,[39−43] the dehydration can also proceed through a two-step mechanism. With respect to the zero-level of **1a**(S_0), the second dehydration step has a barrier of 74.6 kcal/mol[43] that is nearly equal to that on the first step (76.4 kcal/mol). This value is a little lower than the barrier (75.8 kcal/mol) for the one-step dehydration.[42] The direct dehydration for acetic acid in the ground state is in competition with the two-step process involving the 1,1-ethenediol intermediate. Reaction 3, 4, 5, and 6 may take place along the ground-state pathways, but no potential barrier was found above the endothermic character. The separated CH_3 and HOCO or CH_3CO and OH were considered as a supermolecule and the dissociation energies for reaction 3 and 4 were calculated to be 102.3 and 96.3 kcal/mol, respectively. The calculated values are close to those found from heats of formation at 0 K taken from ref 53.

B. Dissociation in the Lowest Triplet State. In this section we investigate reactions that may take place along the lowest triplet state (T_1) pathways. The CAS(8,7) calculated molecular orbitals and their populations clearly show that the lowest triplet state comes from a promotion of a nonbonding electron localized on the O3 atom to the C=O π^* orbital. Thus, T_1 has a $^3n\pi^*$-state character. The electronic rearrangements induced by excitation significantly influence the structure of acetic acid. As discussed previously, CH_3COOH in the ground state has C_s symmetry with all the heavy (C and O) atoms in the symmetric plane. An electronic excitation from S_0 to T_1 results in a rehybridization of the C2 atom from sp^2 to sp^3. As a result, the backbone of the heavy atoms in T_1 becomes pyramidal in structure. The T_1 geometry is depicted in Figure 1, along with the key parameters from the CAS(8,7)/cc-pVDZ calculations. The T_1 minimum was also optimized at the MP2/cc-pVDZ level of theory. The MP2 bond lengths are nearly equal to those from the CAS(8,7) calculations. There are slight differences in the MP2 and CAS(8,7) bond angles. The largest change is associated with the H5−O4−C2−O3 dihedral angle that varied from the CAS(8,7) value of 67.2° to the MP2 value of 82.4°. Similarly, the pyramidal T_1 structure was found for CH_3CHO[21] with the H−C−O−C dihedral angle of about 120.0° and the C−O bond length of about 1.33 Å. In fact, the T_1 or S_1 state has a common pyramidal equilibrium geometry for a wide variety of aliphatic carbonyl molecules.[21,54−56] The adia-

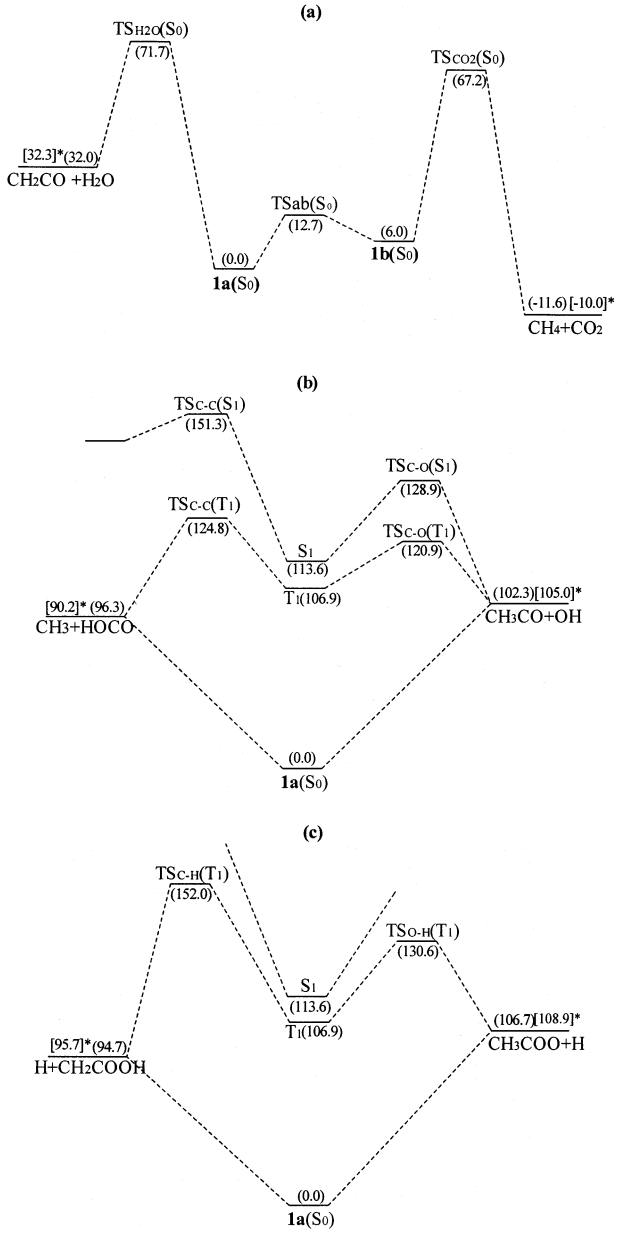

FIGURE 2. Schematic potential energy surfaces of the dissociation processes occurring in the different electronic states: (a) unimolecular reactions in the ground state; (b) the C−C and C−O α cleavages; (c) elimination of hydrogen atom. Relative energies are given in parentheses (in kcal/mol). Dissociation energies in square brackets calculated from the heats of formation in ref 51 are labeled with a star.

(53) Lias, S. G.; Bartmess, J. E.; Liebman, J. F.; Holmes, J. L.; Levin, R.; Mallard, W. G. *J. Phys. Chem. Ref. Data, Suppl. 1* **1988**, 17.

(54) Diau, E. W.-G.; Kotting, C.; Zewail, A. H. *ChemPhysChem* **2001**, *2*, 273. Diau, E. W.-G.; Kotting, C.; Zewail, A. H. *ChemPhysChem* **2001**, *2*, 294 and references therein.

(55) Fang, W.-H.; Liu, R.-Z. *J. Chem. Phys.* **2001**, *115*, 5411. Fang, W.-H.; Liu, R.-Z. *J. Chem. Phys.* **2001**, *115*, 10431.

batic excitation energy from S_0 to T_1 was calculated to be 106.9 and 107.8 kcal/mol at the CAS(8,7) and MP2 levels of theory, respectively. On the basis of the CAS(8,7) structures, the CAS+1+2 calculations give a value of 103.8 kcal/mol for the adiabatic excitation energy, with the CAS(8,7) vibrational zero-point energy correction. These results show that dynamic electron correlation has a little influence on the CAS(8,7) calculated relative energies.

The OH radical has a $^2\Pi$ ground state, which divides into $^2A'$ and $^2A''$ states in the C_s point group. The CH_3CO radical in the ground state has a symmetry of $^2A'$, which is nondegenerate. Considering the spin and space symmetries, the two radicals can correlate adiabatically with two singlet and two triplet states (S_0, S_1, T_1, and T_2) of acetic acid, when they approach each other along the C_s or C_1 pathway. This can be seen from Figure 2b, where the T_2 state is not given. At the CAS(8,7)/cc-pVDZ level, the C−OH bond length is 1.340 Å in the **1a**(S_0) structure, while it becomes 1.362 Å in the T_1 minimum. A significant increase in the C−OH bond length gives us a hint that reaction 3 proceeds more easily along the T_1 pathway than on the S_0 surface. A transition state, TSc-o(T_1) in Figure 1, was found on the T_1 surface by the CAS(8,7) calculations. In addition to the O3 nonbonding and C=O π orbitals that are doubly occupied, the active space of TSc-o(T_1) has one orbital with one-electron density of 1.92. This orbital can be approximately represented as 0.4 $2p_x$(C2) + 0.5 $2p_x$(O3) − 0.3 $2p_x$(O4) − 0.3 $2p_y$(C2) − 0.2 $2p_y$(O3) + 0.5 $2p_y$(O4). It is evident that it is a bonding orbital with some antibonding character between the C2 and O4 atoms. The two singly occupied active orbitals are mainly composed of 2p orbitals of C2, O3, and O4 atoms. They have antibonding character between the C2 and O4 atoms. The remaining two active orbitals are nearly empty with one-electron density less than 0.08, but they have some bonding character between the C2 and O4 atoms.

The C−OH separation of 1.725 Å predicts that the C−O bond is partially broken in TSc-o(T_1), and the IRC calculations confirm that TSc-o(T_1) is the transition state on the pathway from CH_3COOH (T_1) to CH_3CO ($^2A'$) and OH ($^2\Pi$). The barrier height is computed to be 14.0 kcal/mol at the CAS(8,7)/cc-pVDZ level of theory with the zero-point energy correction included. TSc-o(T_1) was re-optimized with the MP2/cc-pVDZ method. The resulting barrier of 12.9 kcal/mol is close to the value from the CAS(8,7)/cc-pVDZ calculations. The barrier height was predicted to be 12.3 kcal/mol by the CAS+1+2 single-point energy calculations with the CAS(8,7)/cc-pVDZ zero-point energy correction. All of these provide evidence that dynamic electron correlation has a small influence on the CAS(8,7) calculated barrier height.

Another important pathway for CH_3COOH decomposition in the T_1 surface involves breaking the C−C bond (namely reaction 4). In the ground state, the α-C−OH bond is stronger than the α-C−C bond, mainly because of conjugation interaction between the $2p_z$ electrons of O4 and the C=O π electrons. In the T_1 state, the C−OH bond length is significantly increased due to the absence of the conjugation interaction, while the C−C bond is only slightly lengthened with respect to that in the ground state. Cleavage of the C−C bond may be in competition with the C−OH bond breaking in the T_1 state. A transition state of TSc-c(T_1) was obtained and confirmed to be the first-order saddle point governing CH_3COOH (T_1) dissociation to the ground-state fragments of CH_3 ($^2A_2''$) and HOCO ($^2A'$). With respect to the T_1 minimum, the barrier height is 20.0 kcal/mol at the CAS(8,7)/cc-pVDZ level of theory. It becomes 17.9 kcal/mol when the vibrational zero-point energy correction is included. This barrier is reduced to 13.1 kcal/mol by the CAS+1+2 calculations. Comparison of this value to the barrier of 12.3 kcal/mol found for the C−OH bond cleavage pathway indicates a small preference for reaction 3 to proceed on the T_1 surface. The three active orbitals for TSc-c(T_1), which are almost doubly occupied, are nearly the same as those for TSc-o(T_1). The two unpaired electrons have large probability in the C1 and O3 atoms, but are considerably delocalized into the C2 and O4 atoms. One vacant active orbital has partially bonded character between the C1 and C2 atoms, while the other vacant active orbital has partial bonding character between the C2 and O3 atoms. The CASSCF molecular orbitals and their populations give evidence that the C−C σ bond is mainly broken in the TSc-c(T_1) structure.

Dissociation reactions 5 and 6 may proceed along the T_1 surface. Two transition states, referred to as $TS_{O-H}(T_1)$ and $TS_{C-H}(T_1)$ in Figure 1, were found on the T_1 surface. The displacement vectors associated with the imaginary modes show that $TS_{O-H}(T_1)$ and $TS_{C-H}(T_1)$ are the transition states which govern the CH_3COOH (T_1) dissociation to CH_3COO + H and H + CH_2COOH, respectively. Further evidence for this comes from the O−H separation of 1.343 Å in $TS_{O-H}(T_1)$ and the C−H separation of 1.768 Å in $TS_{C-H}(T_1)$. The potential energy profiles for reactions 5 and 6 are plotted in Figure 2c. Since the barrier heights of 23.6 kcal/mol for reaction 5 and 45.1 kcal/mol for reaction 6 are much higher than those for reactions 3 and 4, the elimination reactions involving the hydrogen atom are not in competition with the α-cleavage reactions of CH_3COOH (T_1) on the T_1 surface.

C. Dissociation in the First Excited Singlet State. The S_1 minimum of acetic acid was optimized at the CAS(8,7)/cc-pVDZ level of theory and was confirmed by the calculated vibrational frequencies which were all real. The CASSCF wave functions and natural orbital population show that the S_1 state is reached by one-electron excitation from the n orbital to the C=O π^* orbital. As in the T_1 state, this excitation causes pyramidalization of the backbone of the heavy atoms, resulting in a C_1-symmetry equilibrium geometry shown in Figure 1. The adiabatic and vertical excitation energies from S_0 to S_1 are computed to be 113.6 and 148.4 kcal/mol, respectively, at the CAS(8,7)/cc-pVDZ level, and 108.5 and 145.0 kcal/mol, respectively, at the CAS+1+2 level. Comparison with photodissociation experiments at wavelengths in the 200−222-nm region (which correspond to the vertical excitation energy in the range from 128.8 to 143.0 kcal/mol) shows that the present computations provide a reasonable value for the adiabatic excitation energy, and may overestimate the vertical excitation energy by a few kcal/mol. Although the T_1 and S_1 states come from the same electronic configuration ($n^1\pi^{*1}$), their equilibrium structures are considerably different. The C2−O3 bond length in S_1 is 1.415 Å, which is 0.024 Å longer than that

(56) Chen, X.-B.; Fang, W.-H. *Chem. Phys. Lett.* **2002**, *361*, 473.

in T_1, while the C1−C2, C2−O4, and O4−H5 bonds are noticeably shorter in the S_1 state with respect to those in the T_1 state. The structural difference between the T_1 and S_1 states predicts that the α-bond cleavage proceeds less easily on the S_1 state than it does on the T_1 state.

Both the T_1 and S_1 states of acetic acid correlate adiabatically with the ground-state fragments of CH_3CO ($^2A'$) and OH ($^2\Pi$). One can expect that the $TS_{C-O}(S_1)$ structure is similar to that of $TS_{C-O}(T_1)$. The active space used for the CAS(8,7) optimization of $TS_{C-O}(S_1)$ is nearly the same as that for $TS_{C-O}(T_1)$. The transition state [$TS_{C-O}(S_1)$] for the C2−O4 bond cleavage in S_1 is shown in Figure 1 along with the key bond parameters. Since the C2−O4 bond is nearly broken in $TS_{C-O}(T_1)$ or $TS_{C-O}(S_1)$, the OH group can move freely, which causes little change in the energy of the system. Thus, a large difference exists in the orientation of the OH group relative to the CH_3CO moiety. An imaginary frequency of 1029.8(i) cm^{-1} was found for the $TS_{C-O}(S_1)$ structure by vibrational analysis. The eigenvector corresponding to the negative eigenvalue of the force constant matrix indicates that the internal coordinate reaction vector is mainly composed of the C2−O4 bond cleavage and some changes in the C2−O3 bond length and the O3−C2−C1 and O4−C2−C1 angles. The reaction vector has been identified as $-0.35R_{C2-O3} + 0.83R_{C2-O4} + 0.23A_{O3-C2-C1} - 0.24A_{O4-C2-C1}$. It is obvious that $TS_{C-O}(S_1)$ is the transition state governing the CH_3COOH (S_1) dissociation into CH_3CO ($^2A'$) and OH ($^2\Pi$). Relative to the S_1 minimum, the barrier height is 15.3 kcal/mol at the CAS-(8,7)/cc-pVDZ level, with the CAS(8,7)/cc-pVDZ zero-point correction included. The barrier height is nearly unchanged with the CAS+1+2 calculations (15.4 kcal/mol), but is a little higher than that found on the T_1 pathway. Guest and co-workers[11−13] noted that the most likely dynamical origin of the high product translation for acetic acid photolysis was a barrier to product formation in the decomposition exit channel. The barrier height is equivalent to the activation energy required for the recombination of the products, CH_3CO ($^2A'$) and OH ($^2\Pi$), and conversely is approximately the translational energy released in the dissociation. Experiments at 218 and 200 nm produced almost identical mean translational energy of 13.9 kcal/mol and indicate the exit barrier is 13−14 kcal/mol. The calculated barrier height for the C−O cleavage is in good agreement with the experimental estimation.[11−13]

The CH_3 radical has a ground state of $^2A_2''$, while the ground state of HOCO is $^2A'$. When the two ground-state radicals approach each other with either C_s or C_1 symmetry, they can correlate adiabatically with the ground and lowest triplet states of CH_3COOH. Therefore, acetic acid in the S_1 state can only correlate with an excited electronic state of the fragments of CH_3 and HOCO. The transition state of $TS_{C-C}(S_1)$ was found and confirmed to be the first-order saddle point on the S_1 surface. The C−C separation in $TS_{C-C}(S_1)$ is 0.17 Å longer than that in $TS_{C-C}(T_1)$, but the largest difference in their structures is associated with the O4−C2−O3 angle that changes from 118.9° in $TS_{C-C}(T_1)$ to 144.3° in $TS_{C-C}(S_1)$. In the ground state of the HOCO radical, the O−C−O angle is about 120°, due to the sp^2 hybridization of the C atom. One electron is promoted from the nonbonding orbital localized at the C atom to the C=O π^* orbital, which results in a rehybridization of the C atom from sp^2 to sp. As a consequence, the HOCO radical in its excited state ($^2A''$) has an O−C−O configuration close to linearity (the O−C−O angle in the HOCO ($^2A''$) structure was predicted to be 174.4° by the CCSD(T)/cc-pVTZ calculations[57]). This leads us to expect that $TS_{C-C}(S_1)$ is the transition state governing the CH_3COOH (S_1) dissociation to CH_3 ($^2A_2''$) and HOCO ($^2A''$). The CAS(8,7)/cc-pVDZ calculations provide a barrier of 37.7 kcal/mol for the dissociation, which becomes 36.8 kcal/mol by the CAS+1+2 calculations. This barrier is much higher than the corresponding one on the T_1 surface. The relatively high barrier to the C−C bond cleavage on the S_1 surface originates from the fragment of HOCO in the excited electronic state ($^2A''$), which has an energy of about 70.7 kcal/mol[57] above the zero level of the ground state. Similarly, high barriers were found for reactions 5 and 6 on the S_1 surface, since they adiabatically correlate with the excited-state fragments. These two reactions are not further investigated here.

D. Surface Intersections and Mechanistic Aspects. Photodissociation of acetic acid is likely nonadiabatic. The reaction starts on one excited state and may proceed along another excited or ground state pathway. Therefore, intersection of the surfaces probably plays an important role in the CH_3COOH photodissociation. The minimum-energy crossing point between S_1 and T_1 surfaces was optimized at the level of SA-CAS(8,7)/cc-pVDZ with different initial geometries. The resulting structure was labeled as S_1/T_1 in Figure 1. With respect to the S_1 minimum, the S_1/T_1 crossing point has an energy of 6.3 kcal/mol. The bond parameters of the S_1/T_1 and S_1 structures in Figure 1 show that the two structures are similar to each other. The S_1/S_0 minimum-energy crossing point was optimized at the SA-CAS(8,7)/cc-pVDZ and SA-CAS(10,8)/cc-pVDZ levels with the C2−O3 σ and σ^* orbitals included in the active space. But the S_1/S_0 structure could not be completely optimized with the maximum force of about 0.002 hartree/bohr. Although there are some uncertainties in the S_1/S_0 structure and energy, we can say that the S_1/S_0 intersection is far from the Franck−Condon region with relatively high energy. Relative to the S_1 minimum, energies of the S_1 and S_0 states at the S_1/S_0 point are respectively 39.1 and 36.3 kcal/mol at the SA-CAS(8,7)/cc-pVDZ level. The S_1/S_0 structure is depicted in Figure 1, along with the SA-CAS-(8,7)/cc-pVDZ bond parameters.

As observed in experiments, photoexcitation in the region of 200−222 nm corresponds to the n−π^* transition, which results in the CH_3COOH molecules being transferred to the first excited singlet state (S_1). From this state there are three possible radiationless routes for CH_3COOH (S_1) to deactivate: internal conversion (IC) to the ground state, intersystem crossing (ISC) to the lowest triplet state, and direct dissociation on the S_1 surface. The S_1/S_0 structure is quite different from that of the S_1 minimum. The S_1/S_0 crossing point is 32.8 kcal/mol in energy higher than the S_1/T_1 point and 23.8 kcal/mol above the saddle point for the α-cleavage of the C−O bond. In addition, the S_1/S_0 point is nearly inaccessible in energy, even with photoexcitation at 200 nm. The IC

(57) Duncan, T. V.; Miller, C. E. *J. Chem. Phys.* **2000**, *113*, 5138. Li, Y.; Francisco, J. S. *J. Chem. Phys.* **2000**, *113*, 7963.

from S_1 to S_0 would be expected to have less probability compared with ISC to T_1 or direct dissociation on the S_1 surface. Experimental investigations[12,13,16,17] provide unequivocal evidence for the presence of an energy barrier in the exit channel leading to $CH_3CO + OH$ products. The present ab initio calculations suggest that the barrier to the C−OH fission exists on the T_1 or S_1 pathway, but not on the ground-state surface. Thus, the IC to the ground state is unlikely to provide the route for the S_1 state parent molecules to dissociate to ground-state radical products of $CH_3CO + OH$.

It is possible for reactions 3−6 to proceed on the S_1 surface. But the latter three reactions are not in competition with the first one, due to high barriers on the S_1 pathways for reactions 4−6. The α-C−O bond cleavage, reaction 3, has a barrier of only 15.3 kcal/mol on the S_1 surface. After photoexcitation at 200−222 nm, the CH_3-COOH molecules in S_1 have enough internal energy to overcome the barrier to produce CH_3CO ($^2A'$) and OH ($^2\Pi$) fragments. Therefore, direct dissociation on the S_1 surface is one of the important pathways for generating OH ($^2\Pi$) radicals.

The structural similarity between the S_1/T_1 point and the S_1 minimum suggests that ISC from S_1 to T_1 can occur to a noticeable extent. Further evidence that the ISC process can occur to an appreciable extent comes from the calculated spin−orbit coupling (SOC) constant between the S_1 and T_1 surfaces (which is 68.2 cm^{-1} at the S_1/T_1 point). The S_1/T_1 point can be considered as a "transition state" of the nonadiabatic process from S_1 to T_1, the barrier of 6.3 kcal/mol is 9.0 kcal/mol lower than that for the S_1 direct dissociation to CH_3CO ($^2A'$) and OH ($^2\Pi$). However, the $S_1 \rightarrow T_1$ ISC is a spin-forbidden process, which has a probability factor of less than 1. If the spin-forbidden process is treated as a spin-allowed process, the rate calculated with the transition state theory will be reduced significantly. The present calculations indicate that the ISC from S_1 to T_1 process is in competition with the S_1 direct dissociation reaction.

Hydrogen elimination from the terminal CH_3 group of acetic acid is almost impossible on the T_1 surface, due to a very high barrier to this reaction. The elimination of hydrogen from the O−H group might take place, but cannot realistically compete with the α-cleavage reactions on the T_1 surface. Once the CH_3COOH molecules are on the T_1 surface, they dissociate either to CH_3CO ($^2A'$) and OH ($^2\Pi$) or to CH_3 ($^2A_2''$) and HOCO ($^2A'$), but the former has a small preference over the latter. The fragments CH_3 ($^2A_2''$) and HOCO ($^2A'$) have been observed in a study[58] of the HOCO radical from the CH_3COOH photodissociation. HOCO is the intermediate of the $OH + CO \rightarrow H + CO_2$ reaction that is important in combustion.[59,60] The structures, reactivity, and spectra of HOCO and its isomer HCO_2 have been investigated theoretically and experimentally.[57,61,62]

Since the CH_3COOH molecules in S_1 correlate with the excited-state fragments of CH_3 ($^2A_2''$) and COOH ($^2A''$) and a high barrier exists on the S_1 path, the C−C bond breaking takes place only after intersystem crossing to the T_1 surface. The barrier to the T_1 dissociation is 17.9 kcal/mol for formation of CH_3 ($^2A_2''$) + HOCO ($^2A'$) and 14.0 kcal/mol for formation of CH_3CO ($^2A'$) + OH ($^2\Pi$). If the C−O α bond cleavage of acetic acid occurs only on the T_1 surface, the relative yields are found to be [OH]:[HOCO] = 5.2:1 by the RRKM calculations[63,64] with use of the CAS(8,7) frequencies for CH_3COOH (T_1), $TS_{C-O}(T_1)$, and $TS_{C-C}(T_1)$ and a vertical excitation energy of 143 kcal/mol (photodissociation at 200 nm). However, only the OH ($^2\Pi$) radicals were observed in some experiments[10−13,16,17] of the CH_3COOH photodissociation, which give additional evidence that the C−O bond fission occurs along the S_1 pathway.

In general, the weaker of the two α-C−C bonds is cleaved preferentially for asymmetrically substituted aliphatic ketones. The usual mechanism involved for α bond fission in carbonyl compounds upon $n \rightarrow \pi^*$ excitation is ascribed to intersystem crossing to the lowest triplet state followed by dissociation on the T_1 surface.[65] Upon nonalkyl substitution the situation becomes more complicated. UV photodissociation of acetyl chloride[45,46,66] shows that cleavage of the C−Cl bond dominates despite both α-bonds having a similar bond energy. The observation of a highly anisotropic angular distribution for photofragments from the acetyl chloride photodissociation at 248 nm leads Butler and co-workers[45,46] to propose a C−Cl α-cleavage mechanism on the S_1 surface. The fast rate for the C−Cl bond fission predicts a very small barrier on the S_1 pathway. A similar situation was been found for acetyl bromide,[67] iodide,[68] and acetyl cyanide.[69−71] The Cl, Br, or I atom, one of the fragments from dissociation of acetyl halide (CH_3COX, X = Cl, Br, and I), is 3-fold degenerate in the ground state (^2P). Qualitatively, the CH_3COX (X = Cl, Br, and I) molecules in S_1 correlate adiabatically with the products of $CH_3CO + X$ in the ground state. Quantitatively, acetyl halides have the repulsive S_1 potential energy surfaces or have very small barriers on the S_1 surfaces that lead to prompt dissociation. The intersystem crossing and other processes are not in competition with the S_1 direct dissociation for acetyl halides.

Acetic acid can be regarded as one of the simplest asymmetrically substituted ketones. The present calculations predict that the C−O single bond cleavage has a barrier of 15.3 kcal/mol on the S_1 surface. The isotropic distribution of the OH ($^2\Pi$) fragment, which has been experimentally observed, is probably a result of this

(58) Sears, T. J.; Fawzy, W. M.; Johnson, P. M. *J. Chem. Phys.* **1992**, *97*, 3996.
(59) Petty, J. T.; Moore, C. B. *J. Chem. Phys.* **1993**, *99*, 47.
(60) Petty, J. T.; Harrison, J. A.; Moore, C. B. *J. Phys. Chem.* **1993**, *97*, 11194.
(61) Schatz, G. C.; Fitzchales, M. S.; Harding, L. B. *Faraday Discuss Chem. Soc.* **1987**, *84*, 359. Kudla, K.; Schatz, G. C.; Wagner, A. F. *J. Chem. Phys.* **1991**, *95*, 1635.
(62) Kim, E. H.; Bradforth, S. E.; Arnold, D. W.; Metz, R. B.; Neumark, D. M. *J. Chem. Phys.* **1995**, *103*, 7801.
(63) Miller, W. H. *J. Am. Chem. Soc.* **1979**, *101*, 6810.
(64) Eyring, H.; Lin, S. H.; Lin, S. M. *Basic Chemical Kinetics*, John Wiley & Sons: New York, 1980.
(65) Turro, N. J. *Modern molecular photochemistry*; University Science Books; Mill Valley, CA, 1991. Calvert, J. G.; Pitts, J. N., Jr. *Photochemistry*; Wiley: New York, 1966.
(66) Arunan, E. *J. Phys. Chem. A* **1997**, *101*, 4838.
(67) Lane, I. C.; Meehan, R.; Powis, I. *J. Phys. Chem.* **1995**, *99*, 12371.
(68) Kroger, P. M.; Riley, S. J. *J. Chem. Phys.* **1977**, *67*, 4483.
(69) North, S. W.; Marr, A. J.; Furlan, A.; Hall, G. E. *J. Phys. Chem. A* **1997**, *101*, 9224.
(70) Horwitz, R. J.; Francisco, J. S.; Guest, J. A. *J. Phys. Chem. A* **1997**, *101*, 1231.
(71) Furlan, A.; Scheld, H. A.; Huber, J. R. *J. Phys. Chem. A* **2000**, *104*, 1920.

barrier on the S_1 exit channel for the C−O bond fission. Photoexcitation (in the 200−222-nm region) of acetic acid to the S_1 state leads to dissociation to CH_3CO ($^2A'$) and OH ($^2\Pi$) fragments as the main channel. Meanwhile, the C−C bond fission occurs as a result of intersystem crossing from S_1 to T_1. This is a little different from the photodissociative mechanism of acetyl halide, where only the S_1 direct dissociation can take place. The fragments of CH_3, CHO, and CH_3CO are nondegenerate in the ground state. When CH_3 and CHO or CH_3 and CH_3CO approach each other in C_s or C_1 symmetry, they can correlate adiabatically with CH_3CHO or CH_3COCH_3 in the ground and triplet states. Qualitatively, CH_3CHO or CH_3COCH_3 in the S_1 state only can correlate adiabatically with the fragments in an excited electronic state. The S_1 direct dissociation is difficult for CH_3CHO or CH_3COCH_3, due to high barrier or endothermic character. Experimentally and theoretically, it has been well-established that the mechanism involved for α bond fission in CH_3CHO and CH_3COCH_3 upon n→π^* excitation is intersystem crossing to the lowest triplet state followed by dissociation on the T_1 surface.[21,54,72]

Summary

The potential energy surfaces of the ground state (S_0), the lowest triplet state (T_1), and the first excited singlet state (S_1) for acetic acid dissociation have been mapped with different ab initio methods and the cc-pVDZ basis set. The most probable mechanisms leading to photoproducts were determined through the computed potential energy surfaces and the surface crossing points. The CH_3COOH molecules are populated in the first excited singlet state (S_1) by photoexcitation using wavelengths in the range of 200−222 nm. From this state there are three possible radiationless routes for CH_3COOH (S_1) to deactivate: internal conversion (IC) to the ground state, intersystem crossing (ISC) to the lowest triplet state, and direct dissociation on the S_1 surface. The S_1/S_0 point has a very high energy so the IC process to S_0 has a very small probability to occur compared to the ISC process or direct dissociation occurring on the S_1 surface. Photoexcitation of the CH_3COOH molecules to the S_1 state using 200−222-nm light provides enough internal energy to overcome the barrier of 15.3 kcal/mol to produce the CH_3CO ($^2A'$) and OH ($^2\Pi$) fragments. Direct dissociation on the S_1 surface is one of the important pathways for formation of the OH ($^2\Pi$) radicals following UV photoexcitation of gas-phase acetic acid.

The ISC from S_1 to T_1 is in competition with the S_1 direct dissociation. After intersystem crossing to the T_1 surface, the C−O α bond cleavage occurs preferentially to a small extent compared to breaking the C−C bond. The OH ($^2\Pi$) radicals can be formed via two pathways:

$$\begin{array}{c} CH_3COOH(S_0) + h\nu \rightarrow CH_3COOH(S_1) \rightarrow TS_{C\text{-}O}(S_1) \rightarrow CH_3CO(^2A') + OH(^2\Pi) \\ \downarrow \qquad\qquad\qquad\qquad\qquad\qquad \uparrow \\ ISC \rightarrow CH_3COOH(T_1) \rightarrow TS_{C\text{-}O}(T_1) \end{array}$$

This is the reason the predominant product channel was observed to be CH_3CO ($^2A'$) and OH ($^2\Pi$). The C−C α cleavage takes place only after intersystem crossing to the T_1 surface

$$\begin{array}{c} CH_3COOH(S_0) + h\nu \rightarrow CH_3COOH(S_1) \rightarrow ISC \rightarrow CH_3COOH(T_1) \\ \qquad\qquad\qquad\qquad\qquad\qquad\qquad\qquad \downarrow \\ CH_3\,(^2A_2'') + HOCO\,(^2A') \leftarrow TS_{C\text{-}C}(T_1) \end{array}$$

This reaction has been used to generate the HOCO ($^2A'$) radical, although it is a poorer source for the HOCO ($^2A'$) species with respect to the photodissociation of acrylic acid. An isotropic distribution of fragments for the C−O bond fission was observed for acetic acid photodissociation. The isotropic distribution of the fragments is probably a result of a barrier (15.3 kcal/mol) on the S_1 exit channel.

Carbonyl compounds are likely to undergo the α-bond cleavage upon n→π^* excitation. In this aspect, three types of the aliphatic carbonyl compounds can be distinguished. First are acetyl halides (CH_3COX, X = Cl, Br, and I) whose α-bond cleavage along the S_1 pathway is an exclusive channel following n→π^* excitation. The second category is made up of acetone, acetaldehyde, and so on. The C−C and C−H α bond cleavages for them take place only after intersystem crossing from S_1 to T_1. Upon n→π^* excitation, acetic acid can dissociate into CH_3CO ($^2A'$) and OH ($^2\Pi$) along the S_1 pathway. Meanwhile, the C−C bond fission occurs as a result of the S_1→T_1 intersystem crossing that is in competition with the S_1 direct dissociation. Acetic acid can be considered as a representation of the third kind of carbonyl compounds. An ab initio study on the bond selective photodissociation of acetyl halides and the related compounds is in progress and will be reported in due course.

Acknowledgment. This work has been supported by the National Natural Science Foundation of China (Grant Nos. 20073005 and 20233020) and the Research Grants Council (RGC) of the Hong Kong S.A.R., China.

Supporting Information Available: The structures and energies of the stationary points reported in the present work. This material is available free of charge via the Internet at http://pubs.acs.org.

JO020356O

(72) Diau, E. W.-G.; Kotting, C.; Solling, T. I.; Zewail, A. H. *ChemPhysChem* **2002**, *3*, 57. Solling, T. I.; Diau, E. W.-G.; Kotting, C.; Feyter, S. D.; Zewail, A. H. *ChemPhysChem* **2002**, *3*, 79 and references therein.